Domain-spatial correlation functions and scaling relations of nucleation and growth in polymer films

Tao Huang, Tomohiro Tsuji, M. R. Kamal, and A. D. Rey*
Department of Chemical Engineering, McGill University, 3610 University Street, Montreal, Quebec, Canada H3A 2B2
(Received 31 March 1997)

A theoretical model of nucleation and growth is presented in terms of a domain-spatial correlation function $G(r,t)$. The domain-spatial correlation function directly explores the transformed volume fraction, the time-dependent domain-size distribution function, and the spatial correlation function of domain core centers, simultaneously throughout the entire process. The scaling relation, $\mathcal{G}(r/R_g(t))=G(r,t)/G(r=0,t)$, where $R_g(t)$ is the location of the first minimum of $G(r,t)$, has been defined and evaluated from experimental data. It is exact for free growth during the postnucleation stage, and it also provides a basis for the interpolation between the impingement stage and the grain structures. [S1063-651X(98)10907-8]

PACS number(s): 64.60.Qb, 61.41.+e, 83.80.Es

Domain growth and the evolution of spatial structures have long received attention in various fields of science [1,2]. Domain growth associated with first-order nonequilibrium phase transformation occurs by spinodal decomposition or nucleation and growth [3,4]. Reasonable agreement between scattering experiments and theory for phase separation and ordering has been achieved in many different materials. In contrast, the details of nucleation and growth are not well established [5]. Experimental results on early stage nucleation and growth in mixtures of low molecular weight compounds [6], colloidal suspensions [7], and polymer blends [8,9] are in qualitative disagreement with classical theory.

Although the Kolmogorov, Johnson-Mehl, and Avrami (KJMA) [10] theory of nucleation and growth predicts the time dependence for the reacted fraction, it does not provide any information on the domain-size distribution. The kinetic studies of first-order phase transitions have been devoted to the characterization and evaluation of correlation functions and their relationship with time-dependent diffraction studies. Sekimoto [11] evaluated an exact expression, deduced by Ohta, Ohta, and Kawasaki in n dimensions [12], for the two-point correlation functions related to the crystallized fraction. Axe and Yamada [13] obtained an expression of the grain autocorrelation function in a one-dimensional system and estimated it by Monte Carlo simulation in two dimensions. They did not consider spatial correlation, which is another very important structural measure for any kind of domain growth or ordering. The above efforts are limited and lack experimental validation.

Polymer nucleation and growth is a first-order phase transition. There are several advantages to studying nucleation and growth phenomena during the postnucleation stage using semicrystalline polymer films. First of all, due to the slow dynamics of polymer crystallization, a deeper quench or larger supercooling ($\Delta T=T_m-T_c \gg 1\sim 10\ ^\circ\mathrm{C}$) is needed for normal nucleation and growth, so that small thermal fluctuations have less effect on the system. Secondly, polymer nucleation and growth is interface kinetics controlled, and growth velocities (about $10^{-3}\sim 10\ \mu$m/sec) are much slower than in diffusion controlled systems, so that higher spatiotemporal resolution can be easily achieved. Thirdly, the nucleation rate, linear growth velocity and geometrical shape of domain growth (polymer spherulites) are easily characterized [14,16]. Also, experimental observation shows that spherulitic domains grow independently from each other, and there is neither Ostwald ripening nor elastic long-range interactions during the nucleation and growth process. The above features of the postnucleation and growth of polymer spherulitic domains simplifies the experimental measurements and theoretical analysis.

In this paper, we present a theoretical model of nucleation and growth in terms of a domain-spatial correlation function $G(r,t)$. This model probes the patterns and spatiotemporal evolution of the nucleation and growth process and agrees with experimental data obtained for nucleation and growth in semicrystalline polymer films. The dynamic domain-spatial correlation function directly and simultaneously explores the transformed volume fraction, the time-dependent domain-size distribution, and the spatial correlation for the entire process.

Experiments were carried out with a common polymer, isotatic polyporpylene (iPP, molecular weight $M_\eta = 250{,}000$). A polymer thin film was formed between two glass slides and by pressing the top slide to form a 10-μm-thick polymer film. A Leitz polarized microscope, equipped with a Leitz hot stage for polymer film solidification was used in the direct observation experiments. In this isothermal solidification study, the temperature is controlled within $\pm 0.1\ ^\circ$C. JAVA-Jandel Scientific's video measurement and image processing system was directly connected to the microscope via a charge-coupled-device camera. We focus on the postnucleation stage, during which the size of the nucleus is greater than 1 μm and visible under the optical microscope for real-time *in situ* observation and accurate real-space measurement. To characterize the experimental data and elucidate the governing scaling laws, we propose a domain-spatial correlation function.

For any droplet pattern, the order parameter is defined as follows:

*Electronic address: bbn5@musicb.mcgill.ca

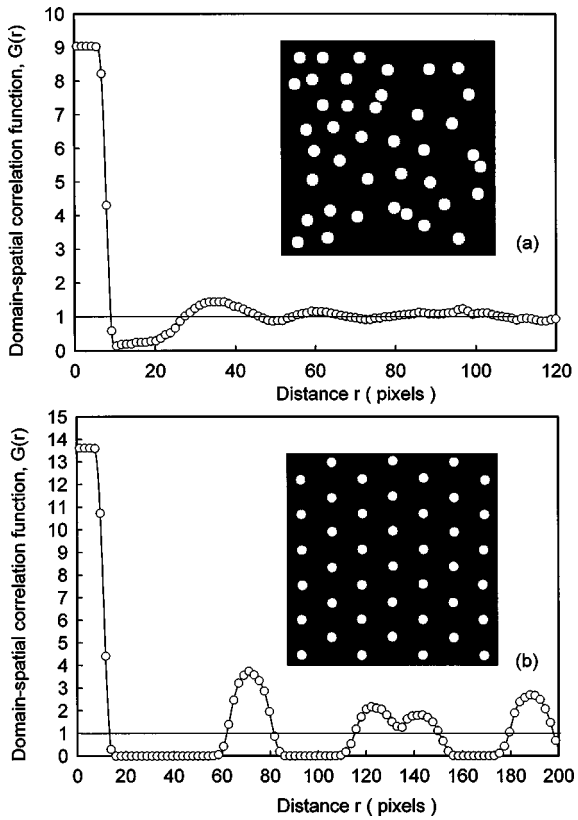

FIG. 1. The static domain-spatial correlation function for equal-size particles where the spatial distributions are the (a) liquidlike state, and (b) solidlike state (hexagonal symmetry).

$$\psi(\vec{\mathbf{x}})=\begin{cases}1 & \text{if } \vec{\mathbf{x}}\in \text{droplet domains},\\ 0 & \text{if } \vec{\mathbf{x}}\ni \text{ droplet domains},\end{cases} \tag{1}$$

where $\vec{\mathbf{x}}$ is the position vector. The new domain-spatial correlation function, for an arbitrarily chosen domain i with $\vec{\mathbf{x}}_i$ as the origin of the domain core center, is found by counting the domains whose position vectors lie within a distance dr from a shell of radius r with center at the origin at time t, which yields

$$G_i(r)=\langle \delta(r-|\vec{\mathbf{x}}_i-\vec{\mathbf{x}}|)\,\psi(\vec{\mathbf{x}})\rangle. \tag{2}$$

Considering the whole system, the domain-spatial correlation function is the ensemble average of this number for all core center positions of over all domains placed at the origin:

$$G(r)=\frac{1}{\rho}\left\langle \sum_i^N \int \delta(r-|\vec{\mathbf{x}}_i-\vec{\mathbf{x}}|)\,\psi(\vec{\mathbf{x}})\,d\vec{\mathbf{x}}\right\rangle, \tag{3}$$

where $\rho=(1/\Omega)\int\psi(\vec{\mathbf{x}})d\vec{\mathbf{x}}$ is the domain density, $\vec{\mathbf{x}}_i$ is the core center position of the domain, Ω is the total geometrical measure in the space, and N is the total number of the domains.

Considering the droplet patterns in which domains are isolated from each other, the static domain-spatial correlation function has the following properties [16]: (1) When $r \ll R_{\max}$, and $R_{\max}$ is the maximum domain size, we get $G(r)=(1/\rho)H(R-r)$ for a monodisperse droplet pattern with radius R, where $H(R-r)$ is Heaviside's step function; and $G(r)=(1/\rho)\int_0^r[1-f(R)]dR$ for a polydisperse droplet pattern with size distribution function, $f(R)$. Therefore, $G(r)$ represents the domain size distribution function when $r<R_{\max}$. (2) When $r\gg R_{\max}$, $G(r)$ represents the spatial correlation function of domains and the peak positions are the same as those of the pair-correlation function of the domain core centers.

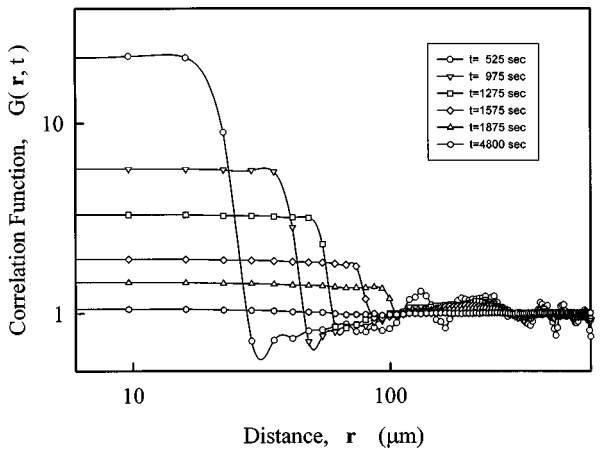

FIG. 2. Dynamic domain-spatial correlation function as a function of distance r, from simultaneous nucleation experiment under isothermal condition; the crystallization temperature is $T_C=140\,^\circ$C. See text.

To evaluate the domain-spatial correlation function (DSCF), Eq. (3), we generate images where the spatial distributions are liquidlike [the inset picture in Fig. 1(a)] and solidlike [the inset picture in Fig. 1(b)] states. Figure 1 shows the corresponding DSCF's. The characteristic features of the DSCF's in Fig. 1(a) are a broad first peak, a smooth second peak, and a third peak with an appreciably diminished intensity, confirming the complete absence of the long-range order, corresponding to a liquidlike state. Figure 1(b) shows that the DSCF's have pronounced peaks at positions corresponding to a hexagonal close-packed (HCP) crystal. A considerably sharper and narrower first peak compared to the liquidlike state, a split in the second peak, and the presence of a distinct third peak in Fig. 1(b) are the characteristic features of a solid state. Also, the periodic distance in peak positions confirms long-range order. The step curves in the left corner of both Fig. 1(a) and Fig. 1(b) show the equal-size distribution.

In the polymer nucleation and growth process, the order parameter is the spherulitic growth domain, thus

$$\psi(\vec{\mathbf{x}},t)=\begin{cases}1 & \text{if } \vec{\mathbf{x}}\in \text{growth domain at time } t,\\ 0 & \text{if } \vec{\mathbf{x}}\in \text{ metastable melt at time } t.\end{cases} \tag{4}$$

Sekimoto indicated that $\psi(\vec{\mathbf{x}},t)$ is connected with the volume fraction of the stable crystallized phase, $\chi(t)$, in KJMA formula [10], which reads as follows [11]:

$$\langle\psi(\vec{\mathbf{x}},t)\rangle=1-\chi(t)=\exp\left(-\int_0^t dt I(t)\Psi(t)\right), \tag{5}$$

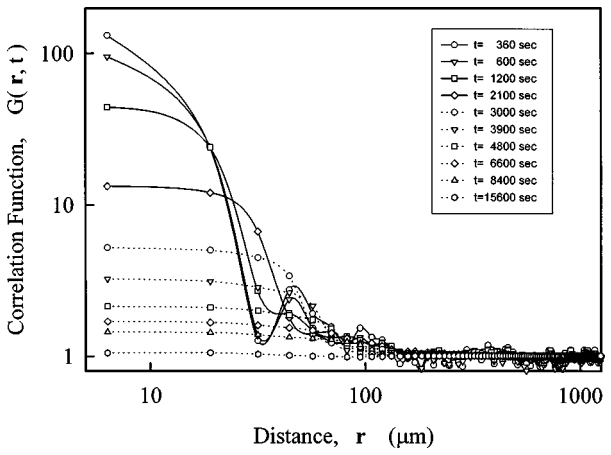

FIG. 3. Dynamic domain-spatial correlation function as a function of distance r, from continuous nucleation experiment under isothermal condition, the crystallization temperature is $T_C = 133\,^{\circ}\mathrm{C}$. See text.

where $I(t)$ is nucleation rate, and $\Psi(t)$ is the volume of the unit hypersphere in the KJMA model. Because the solid fraction changes from zero to one during the transformation, $\psi(\vec{\mathbf{x}})$ is not conserved.

In the simultaneous nucleation case, polymer crystallization involves a constant growth velocity V, and a constant nuclei density I_0. For $r \leqslant R(t)$ and before impingement, the domain-spatial correlation function can be expressed as:

$$G(r,t) = \left[\frac{\exp\left(-\frac{\pi}{3} I_0 V^2 t^3 \right)}{A} \right]^{-1} H(Vt - r). \qquad (6)$$

So, in the free growth stage, $G(r,t)$ is a step function with a width of Vt, and the height of $G(r,t)$ decreases with increasing time. After impingement, there is a mixture of isolated spherulitic domains and some impinged grain islands, and $G(r,t)$ is a step function, representing the equal-size spherulitic domains. It is connected with a smooth oblique curve part that decreases with increasing r, representing the domain-size variation due to impingement.

Figure 2 shows the experimental data involving simultaneous nucleation under isothermal crystallization condition $T_c = 140\,^{\circ}\mathrm{C}$. The data agree with above analysis very well. For $r \leqslant R(t)$ in Fig. 2, the major features are (1) $G(r=0,t)$ is a decreasing function of time because of increasing transformed area, and (2) the step line part of the DSCF becomes larger due to spherulitic domains growth. For $r \gg R(t)$ in Fig. 2, the positions of the first peak and the average interdomain center distance remain unchanged because there are no new domains born during the domain growth process in simultaneous nucleation cases.

In the continuous nucleation case, the growth velocity V is constant during polymer crystallization. The experimental measurement [16] shows that the nucleation rate I agrees with the Kashchiev's nucleation kinetics [17]. For $r \leqslant R_{\max}(t)$ before impingement, the domain-spatial correlation function can be expressed as

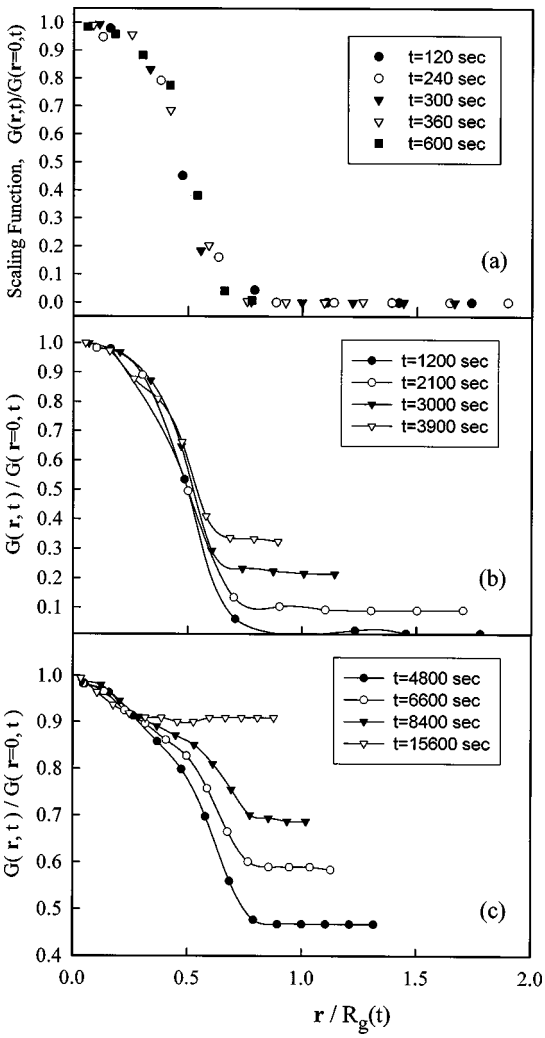

FIG. 4. Experimental results of the scaling relation, $G(r,t)/G(r=0,t)$, as a function of $r/R_g(t)$ from continuous nucleation experiment at isothermal temperature $T_C = 133\,^{\circ}\mathrm{C}$. (a) The early growth during the postnucleation stage shows a perfect scaling relation [see Eq. (8)]; (b) growth and impingement with transformed fraction less than 0.5; the scaling relation is partially obeyed. (c) growth and impingement with transformed fraction greater than 0.5; the scaling relation breaks down in late stages of growth.

$$G(r,t) = \left[\frac{\exp\left(-\frac{\pi}{3} I V^2 t^3 \right)}{A} \right]^{-1} \int_0^r [1 - f(R,t)]\, dR\,. \qquad (7)$$

Figure 3 shows the domain-spatial correlation functions (DSCF) for experiments involving continuous nucleation under isothermal crystallization condition $T_c = 133\,^{\circ}\mathrm{C}$. The left part of Fig. 3 is the smooth curves of the domain-size distribution when $r < R_{\max}(t)$. It represents the growth domains with different sizes and some local impingement structures. The right part of Fig. 3 is the spatial pair-correlation function of domain core centers when $r > R_{\max}(t)$. The first peaks shift slightly to the left with increasing time, which means that the average internuclei distances decrease with increasing time due to the nucleation of new domains. $G(r,t)$ ap-

proaches one in an oscillatory manner at very large r, which means that there is no long-range order.

It is convenient to introduce a scaling relation similar to [13,15]:

$$\mathcal{G}(r/R_g(t))=G(r,t)/G(r=0,t), \tag{8}$$

where $G(r=0,t)=\rho^{-1}$ is the area fraction of transformed grains; and $R_g(t)$ is the location of the first minimum of $G(r,t)$. Figure 4 shows the experimental results of the scaling correlation functions $G(r,t)/G(r=0,t)$ as a function of $r/R_g(t)$; (a) shows that the experimental data superpose when using the scaling relation, Eq. (8), for early growth during the postnucleation stage; (b) shows the case for growth and impingement when the transformed fraction is less than 0.5; and the scaling relation is partially obeyed; (c) shows the case for growth and impingement when the transformed fraction is greater than 0.5, the scaling relation is no longer exact in the late stages of growth, characterized by the emergence of grain structures.

In summary, the above results indicate that the domain-spatial correlation function directly explores the time-dependent domain-size distribution function and the spatial correlation function of domain core centers simultaneously for the entire process, including the postnucleation, domain growth, and grain formation stages. The scaling relation, $G(r,t)/G(r=0,t)$, as a function of $r/R_g(t)$, where $R_g(t)$ is the maximum domain size at time t, has been found from experimental data. It is exact for free growth during the postnucleation stage and also suggests a basis for interpolation between the impingement stage and grain structures. The domain-spatial correlation function and the direct imaging program are suitable to characterize any static droplet patterns and dynamic processes in a wide range of scientific fields.

This work is supported by research grants from the Natural Science and Engineering Research Council of Canada and the Ministére de l'Education, Gouvernement du Québec.

[1] J. W. Evans, Rev. Mod. Phys. **65**, 1281 (1993), and references therein.
[2] D. Stoyan and W. S. Kendall, *Stochastic Geometry and Its Applications* (Wiley, New York, 1995).
[3] J. D. Gunton, M. San Miguel, and P. Sahni, *Phase Transitions and Critical Phenomena*, edited by C. Domb and J. L. Lebowitz (Academic, London, 1983), Vol. 8, p. 267; J. D. Gunton and M. Droz, *Introduction to the Theory of Metastable and Unstable States* (Springer-Verlag, Berlin, 1983).
[4] A. J. Bray, Adv. Phys. **43**, 357 (1994).
[5] J. S. Langer, in *Solids Far From Equilibrium*, edited by C. Godréche (Cambridge University Press, Cambridge, 1989), Chap. 3, p. 297.
[6] S. Krishnamurthy and W. I. Goldburg, Phys. Rev. A **22**, 2147 (1980).
[7] A. Cumming, P. Wiltzius, F. S. Bates, and J. H. Rosedale, Phys. Rev. A **45**, 885 (1992).
[8] K. Schatzel and B. J. Ackerson, Phys. Rev. E **48**, 3766 (1993).
[9] N. P. Balsara, Chenchy Lin, and B. Hammouda, Phys. Rev. Lett. **77**, 3847 (1996).
[10] A. N. Kolmogorov, Bull. Acad. Sci. USSR, Phys. Ser. **1**, 355 (1937); W. Johnson and R. F. Mehl, Trans. Am. Inst. Min. Metall. Pet. Eng. **135**, 416 (1939); M. Avrami, J. Chem. Phys. **7**, 1103 (1939); **X**, 212 (1940), **X**, 177 (1941).
[11] K. Sekimoto, Phys. Lett. A **105**, 390 (1984); J. Phys. Soc. Jpn. **53**, 2425 (1984); Physica A **137**, 96 (1986).
[12] S. Ohta, T. Ohta, and K. Kawasaki, Physica A **140**, 478 (1987).
[13] J. D. Axe and Y. Yamada, Phys. Rev. B **34**, 1599 (1986).
[14] Tao Huang, A. D. Rey, and M. R. Kamal, Polymer **25**, 5434 (1994).
[15] R. Toral, A. Chakrabarti, and J. D. Gunton, Phys. Rev. B **39**, 901 (1989).
[16] Tao Huang, Ph.D. thesis, McGill University, 1997.
[17] D. Kashchiev, Surf. Sci. **14**, 209 (1969).